# Minimization of Intermodulation Distortion in GaAs MESFET Small-Signal Amplifiers

ANDREA M. CROSMUN, MEMBER, IEEE, AND STEPHEN A. MAAS, MEMBER, IEEE

*Abstract* —This paper examines the dependence of third-order intermodulation distortion on the source-reflection coefficient, $\Gamma_s$, as a function of frequency in an amplifier designed according to available-gain criteria. By means of a numerical formulation of the Volterra series, a complete equivalent circuit of the FET can be used, and intermodulation calculations include all feedback effects. We show that the sensitivity of $IP_3$ to $\Gamma_s$ decreases with increasing frequency and can be related to the MESFET's stability.

## I. Introduction

MICROWAVE GaAs MESFET devices are used as amplifiers in a variety of linear applications. However, nonlinear properties of the MESFET's can cause two or more signals applied to the device simultaneously to produce intermodulation (IM) distortion. This distortion has important effects on system performance, particularly in broad-band communication systems. Thus, minimization of IM distortion is often a critical requirement.

In this paper we show how the IM performance of a small-signal amplifier can be optimized when the amplifier is designed according to available-gain criteria. In this process the MESFET's output is conjugate-matched and its input is mismatched to obtain a specified value of gain. We choose this method because it generally results in better dynamic range than do other options; these options are (1) matching the input and mismatching the output or (2) simultaneously matching both the input and output (which, in many cases, is impossible). In available-gain design the value of source impedance that provides the desired gain is not unique and can be selected to optimize IM levels.

In many cases the IM intercept point [1] is a valid figure of merit for IM performance. To obtain the intercept point one must first be able to predict third-order intermodulation products, which result from the nonlinearities in the circuit. Other researchers have attempted to model nonlinearities in GaAs FET's by using the harmonic-balance technique [2]–[4] or specialized, approximate techniques [5]. The Volterra series has also been used to analyze nonlinear distortion in MESFET's [6]–[9]; however, much of this work employs simplifying approximations that reduce accuracy. For example, in the work by Gupta *et al.* [6] the second-degree terms in the Volterra-series expansions were set to zero. However, these second-order products have an effect on the third-order products and therefore must be taken into account. Minasian [7] and Lambrianou *et al.* [8] employ simplified, unilateral equivalent circuits of the MESFET.

These simplifying assumptions are employed to ease the painfully difficult task of generating Volterra kernels in algebraic form. In this work, however, we circumvent such limitations by calculating the kernels numerically; thus, no such simplifying assumptions are necessary, and we can use a complete equivalent circuit of the MESFET. Furthermore, we include the effects of all of the MESFET's feedback elements; these effects have not been examined previously. Because Volterra-series analysis operates entirely in the frequency domain, is noniterative, and requires no convergence process, it is highly efficient and thus is a practical technique for circuit optimization [10].

## II. Modeling the MESFET

This work is based on the packaged Avantek AT10650-5 MESFET, a $0.5\times250$ $\mu m^2$ device that is similar in structure and performance to many commercial *Ku*-band MESFET's. The MESFET chip and its package are modeled by a lumped-element equivalent circuit in which three elements—the gate-to-source capacitance, drain-to-source resistance, and controlled current source—are nonlinear. The modeling process is performed in two steps: first, the equivalent circuit's linear elements are determined and the characteristics of the nonlinear elements are measured. The dependence of the nonlinear elements on voltage is expressed via Taylor-series expansions of their current/voltage ($I/V$) or charge/voltage ($Q/V$) characteristics in the vicinity of their bias points.

The FET's used in this work were taken from a common fabrication lot. $S$-parameter data were measured from 45 MHz to 17 GHz, and several FET's having nearly identical $S$ parameters and $I/V$ characteristics were selected. The high-frequency data covering the range from 2 to 17 GHz were obtained with the transistor biased at a drain voltage of 3.0 V and drain current of 20 mA. The low-frequency $S$ parameters were used primarily to model the drain-to-

Manuscript received December 8, 1988; revised April 20, 1989. This work was supported by the U.S. Air Force Space Division under Contract F04701-88-C-0089.

The authors are with the Aerospace Corporation, P.O. Box 92957, Los Angeles, CA 90009.

IEEE Log Number 8928995.

0018-9480/89/0900-1411$01.00 

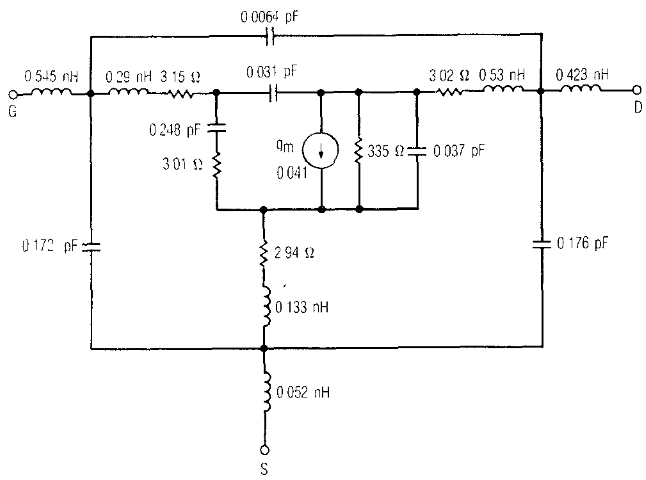


Fig. 1. Linear lumped equivalent-circuit model of the packaged AT10650-5 MESFET.

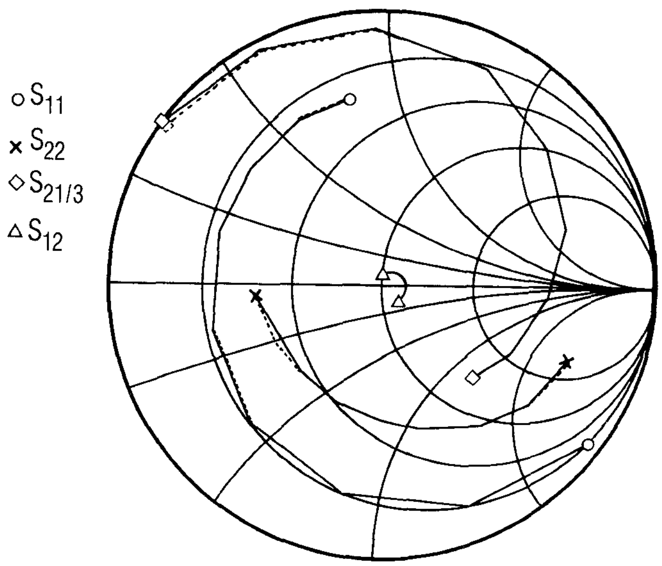


Fig. 2. Measured $S$ parameters of the AT10650-5 MESFET at 3 V, 20 mA bias over the 2–14 GHz range. The solid line represents measured data; the dotted line shows the $S$ parameters calculated from the model in Fig. 1.

source conductance, $G_{ds}$; therefore these were obtained at several bias points near this operating point.

The equivalent-circuit elements were derived from a combination of dc and RF $S$-parameter measurements. Low-frequency $Y$ parameters were used to obtain initial values for some of the elements, and the transconductance was derived from dc measurements. The resistances of the source and drain ohmic contacts were also derived from dc measurements by means of a method similar to that of Yang and Long [11], and modified by Fukai *et al.* [12]. The small-signal linear circuit was then optimized to fit the measured high-frequency $S$ parameters. When an adequate fit to the $S$ parameters was attained, techniques to model the nonlinear elements were employed. The complete model was simply a superposition of the nonlinear elements onto the linear model. The final circuit topology chosen to

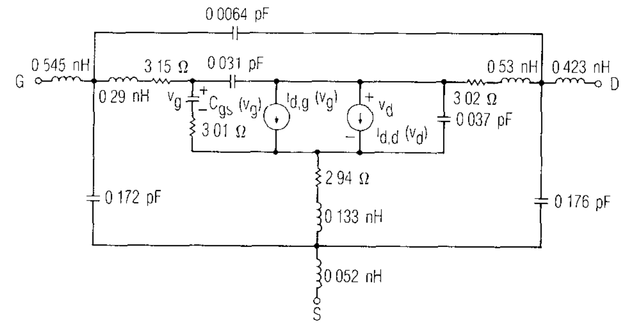


Fig. 3. Nonlinear equivalent circuit of the MESFET in the vicinity of the 3 V, 20 mA bias point. The $i_{d,g}$ coefficients are $a_1 = 0.041$, $a_2 = 0.0171$, $a_3 = -0.0145$; $i_{d,d}$ coefficients are $b_1 = 0.0030$, $b_2 = 3.09 \cdot 10^{-4}$, $b_3 = 3.99 \cdot 10^{-5}$; $V_{g0} = 0.54$ V. $C_{gs}$ is modeled as an ideal Schottky-barrier capacitance; $C_{gs}(0) = 0.331$ pF and its dc bias is $-0.544$ V.

model the packaged device is shown in Fig. 1, and the measured $S$ parameters are compared in Fig. 2 to those of the model.

Modeling the nonlinear transconductance and drain-to-source resistance involves some subtleties. These two elements are derived from a single nonlinear drain-current source, $I_d(V_g, V_d)$, that is controlled by two voltages. In the small-signal case, this current source must be represented by a two-dimensional Taylor series. The small-signal incremental drain current, $i_d(v_g, v_d)$, is

$$\begin{aligned} i_d(v_g, v_d) &= I_d(V_g, V_d) - I_d(V_{g0}, V_{d0}) \\ &= \frac{\partial I_d}{\partial V_g} v_g + \frac{\partial I_d}{\partial V_d} v_d + \frac{1}{2}\left[\frac{\partial^2 I_d}{\partial V_g^2} v_g^2 \right. \\ &\quad \left. + 2\frac{\partial^2 I_d}{\partial V_g \partial V_d} v_g v_d + \frac{\partial^2 I_d}{\partial V_d^2} v_d^2\right] \\ &\quad + \frac{1}{6}\left[\frac{\partial^3 I_d}{\partial V_g^3} v_g^3 + 3\frac{\partial^3 I_d}{\partial V_g \partial V_d^2} v_g v_d^2 \right. \\ &\quad \left. + 3\frac{\partial^3 I_d}{\partial V_g^2 \partial V_d} v_g^2 v_d + \frac{\partial^3 I_d}{\partial V_d^3} v_d^3\right] + \cdots \end{aligned} \tag{1}$$

where $V_{g0}$ and $V_{d0}$ are the bias voltages and $v_g$ and $v_d$ are the incremental gate and drain voltages, respectively, as shown in Fig. 3. In the linear equivalent circuit, the drain current is expressed by the linear terms in (1); thus

$$i_d(v_g, v_d) = \frac{\partial I_d}{\partial V_g} v_g + \frac{\partial I_d}{\partial V_d} v_d \tag{2}$$

or

$$i_d(v_g, v_d) = g_m(V_{g0}, V_{d0}) v_g + G_{ds}(V_{g0}, V_{d0}) v_d \tag{3}$$

and the small-signal drain current can be modeled by means of a pair of separate elements, the controlled source $g_m$ and the controlled conductance $G_{ds}$.

In the nonlinear case the controlled source and conductance are traditionally modeled as two separate nonlinear elements, each controlled by a single voltage; thus

$$i_d(v_g, v_d) = i_{d,g}(v_g) + i_{d,d}(v_d) \tag{4}$$

where

$$i_{d,g}(v_g) = a_1 v_g + a_2 v_g^2 + a_3 v_g^3 \tag{5}$$

and

$$i_{d,d}(v_d) = b_1 v_d + b_2 v_d^2 + b_3 v_d^3. \tag{6}$$

The $a_n$ and $b_n$ coefficients are the $\partial^n I_d/\partial V_g^n$ and $\partial^n I_d/\partial V_d^n$ terms in (1); from (1)–(3), $a_1 \equiv g_m$ and $b_1 \equiv G_{ds}$. This approach is an approximation because it neglects the cross terms $\partial^k I_d/\partial V_g^n \partial V_d^n$ in (1). Although it is clear that the cross terms are usually much smaller than the terms involving $V_g$, they are sometimes not small compared to those involving $V_d$. The terms involving $V_d$ are rarely dominant, but may still be significant; thus, these cross terms may also be significant.

The modeling of $i_{d,g}$ is further complicated by its weak nonlinearity, especially near the bias points that would normally be used for high-dynamic-range amplifiers. Because this nonlinearity is so weak, even small measurement uncertainty and low levels of quantization noise may obscure the curvature in $i_{d,g}$. Even when the noise level is low, the direct differentiation of $i_{d,g}$ to obtain the derivatives in (1) increases the noise level and makes unreliable the derivatives beyond the second. Furthermore, least-square fitting to a polynomial, a commonly used alternative, often fails because the ill-conditioned nature of the normal equation makes the process overly sensitive to small changes in the measured $I/V$ data.

Another problem is the well-known frequency dependence of $G_{ds}$, which is often attributed to traps in the MESFET's channel. These cause the value of $G_{ds}$ measured above 1 MHz to be one fifth to one half the dc value, and to have effects on the higher derivatives $\partial^n I_d/\partial V_d^n$ which are difficult to characterize.

Because of these effects, it is usually not possible to obtain the derivatives in (1) by dc measurements. The cross terms are even more difficult to measure than the others, so there is little choice but to neglect them and to model $i_d(v_g, v_d)$ as two separate, singly controlled nonlinear elements. The consequences of this approach are acceptable in circuits in which $i_{d,g}(v_g)$ is the dominant nonlinearity; this is the case in virtually all modern MESFET's.

These considerations are not unique to Volterra-series analysis. They apply to any form of analysis used to calculate small-signal nonlinear effects in FET amplifiers; in particular, to harmonic-balance analysis. Because harmonic-balance analysis is applied primarily to large-signal circuits, the models usually are designed to describe the MESFET over the entire range of drain-to-source and gate-to-source voltages. However, these models may not accurately express the derivatives in (1) in the vicinity of a specific bias point, and their use may result in incorrect results when applied to small-signal distortion problems.

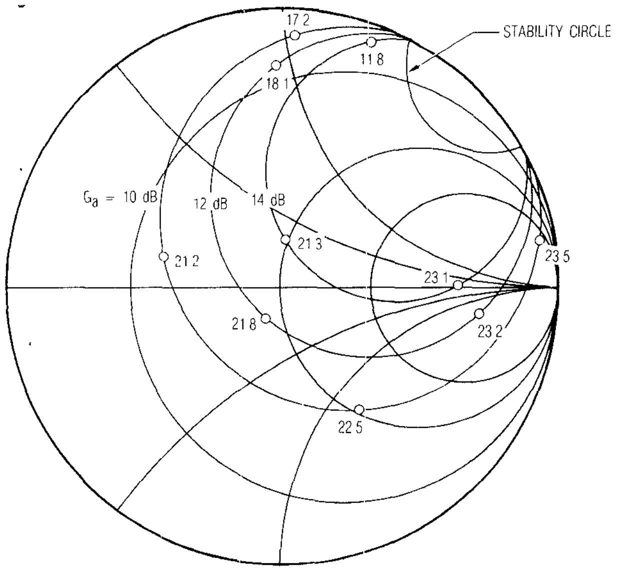


Fig. 4. Gain and stability circles and calculated third-order intercept points of the MESFET at 2 GHz.

The $a_n$ terms in (5), which represent a nonlinear controlled current source, were determined by the method described in [13]. This method involves extracting the source's Taylor-series coefficients from harmonic measurements at low frequencies. The $b_n$ terms in (6) represent a nonlinear conductance. These were found by numerically differentiating values of $G_{ds}$ obtained from low-frequency $Y$ parameters over a range of values of $v_d$; because the curvature of $G_{ds}(V_d)$ was much greater than the uncertainties in the data, and only two derivatives need be taken, a multipoint derivative formula gave good results. Because it is based partly on dc measurements, this process only partially compensates for the frequency sensitivity of $G_{ds}$.

The value of gate capacitance $C_{gs}$ varies with $V_g$, the voltage across the capacitor's terminals. $C_{gs}$ behaves as a uniformly doped Schottky-barrier diode capacitance having the controlling voltage $v_g$, and was modeled as such. The nonlinear MESFET model was established by including the nonlinearity of $C_{gs}$, $G_{ds}$, and $g_m$ in the linear equivalent circuit of Fig. 1. The nonlinear equivalent circuit is shown in Fig. 3.

## III. Calculations

The available gain of a two-port is a function solely of the source reflection coefficient $\Gamma_s$; the locus of $\Gamma_s$ values that provide a specific value of gain lie on a circle in the $\Gamma_s$ plane. The available-gain and stability circles of the GaAs FET were plotted on a Smith chart for three frequencies: 2, 5, and 10 GHz. Intermodulation (IM) products were calculated at points chosen periodically along the gain circles to find values that would maximize the amplifier's third-order intercept point, $IP_3$. The stability circles and the corresponding intercept points are shown in Figs. 4, 5, and 6.

In order to calculate the $IP_3$ values, it was necessary to modify the FET model to account for differences between

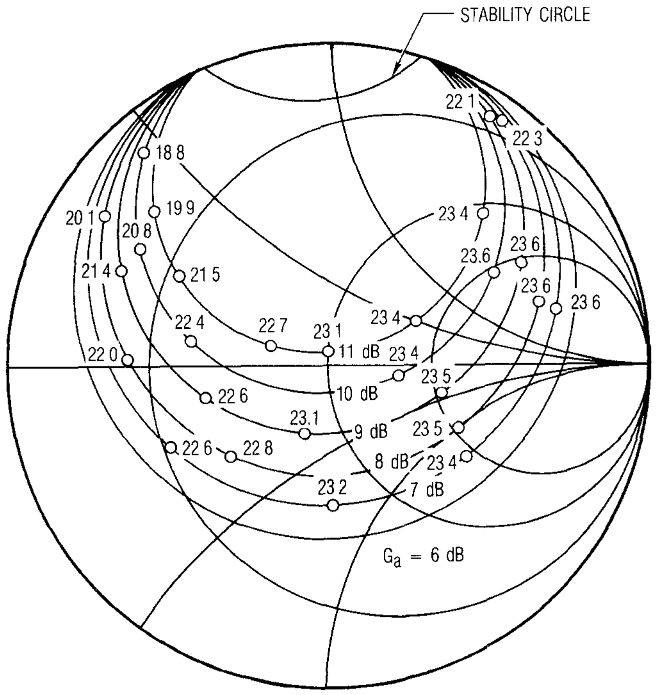


Fig. 5. Gain and stability circles and calculated third-order intercept points of the MESFET at 5 GHz

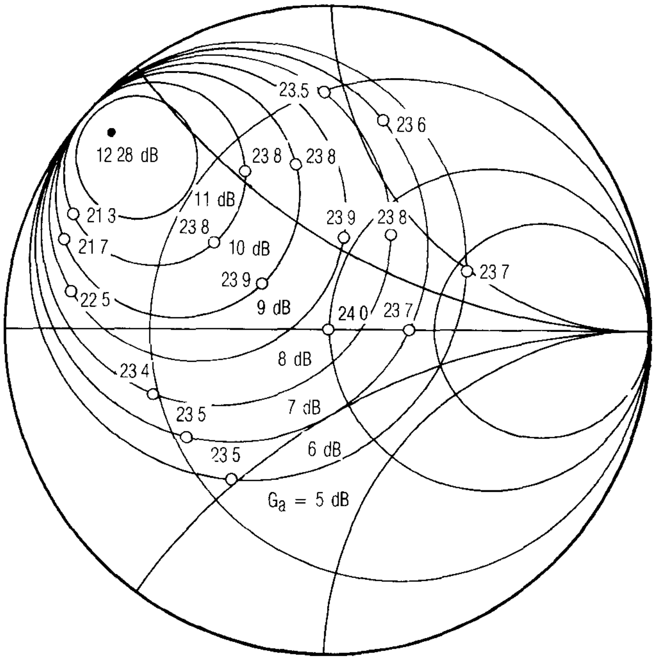


Fig. 6. Gain and stability circles and calculated third-order intercept points of the MESFET at 10 GHz.

the coaxial transistor test fixture (TTF) and microstrip amplifier environments. The TTF measurements included the inductance of a short section of gate and drain leads, and these excess lengths do not exist in the amplifier. The model was therefore modified by taking out these added inductances, and the data shown in Figs. 4 through 6 do not include them.

The process of calculating the intercept points is implemented numerically, and thus is straightforward. In practice it is necessary only to create a data file that describes the circuit elements and their nodal interconnections, along with ancillary information such as frequencies and the mixing product of interest (the data file is similar in appearance to that of nodal-entry linear circuit-analysis programs). The element catalog includes both lumped and distributed elements, including a microstrip model that accounts for loss and dispersion. It is necessary, in the case of nonlinear elements, to include the Taylor-series coefficients, although the program can generate them for elements having well-established nonlinear characteristics (e.g. diode-junction conductance and capacitance). Arbitrary source- or load-impedance data are entered via a disk file. The program requires only a few seconds per data point when used on an 8 MHz IBM PC-AT computer.

The program is based on an implementation of the Volterra series called the *method of nonlinear currents* [1]. This method converts the weakly nonlinear circuit into a linear circuit and a set of current sources whose currents are, at each order, a function of all lower order node voltages. The program operates by first determining the linear, or first-order, voltages at each of the circuit's nodes. It then uses these voltages to generate excitation-current sources at the second-order mixing frequencies; each nonlinear element is replaced by one such source. The remainder of the circuit is linear, and can be solved to obtain second-order voltages by conventional nodal methods. Similarly, the third-order mixing products are found from the first- and second-order products. The method includes the effects of all lower order mixing products on each higher order mixing product.

## IV. Results

The intercept points calculated for the 10 GHz and 5 GHz amplifier gain circles were verified experimentally by measuring the IM levels of several amplifiers designed at these frequencies. Because the IM levels were relatively independent of $\Gamma_s$ at 10 GHz, only the point $\Gamma_s = 0$ was tested, with the load reflection coefficient $\Gamma_L$ equal to zero and a conjugate match. For the 5 GHz case, however, several configurations were built and tested in an attempt to cover the range of values of $\Gamma_s$ that displayed significant variation in IM level.

For the first 10 GHz case an amplifier was built with $\Gamma_s, \Gamma_L = 0$. The measured gain of this amplifier was 4.5 dB, and the intercept point was found to be 22.4 dBm. The calculated values were 5.0 dB and 20.9 dBm, respectively. With the output conjugately matched, the gain improved to 6.8 dB and the output intercept point was 23.5 dBm. Calculated values under these conditions were 6.1 dB and 24.1 dBm, respectively.

To verify the 5 GHz theoretical results, several points in the $\Gamma_s$ plane were tested experimentally. These tests required an amplifier whose input matching circuit could have a range of $\Gamma_s$ values (from the worst to the optimum intercept-point locations) on various gain circles. This in-

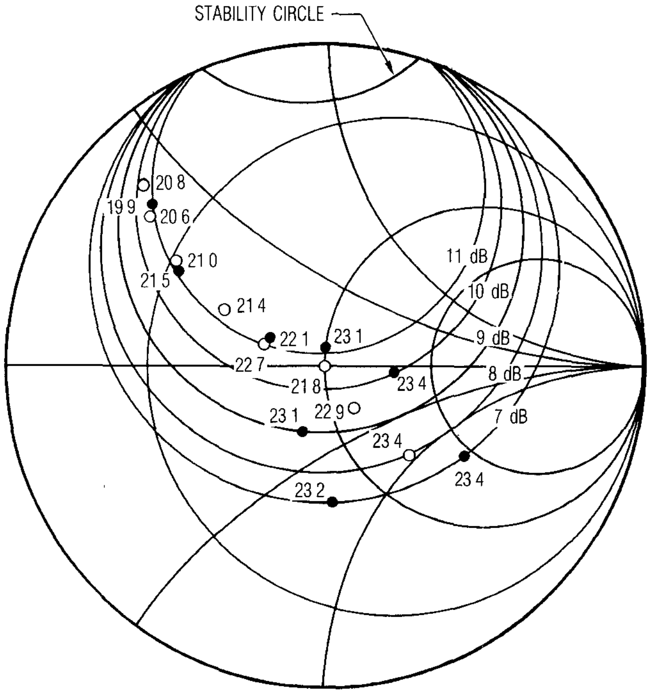


Fig. 7. Gain and stability circles and third-order intercept points of the MESFET at 5 GHz. Measured $IP_3$ values are indicated by circles, calculated values by solid dots.

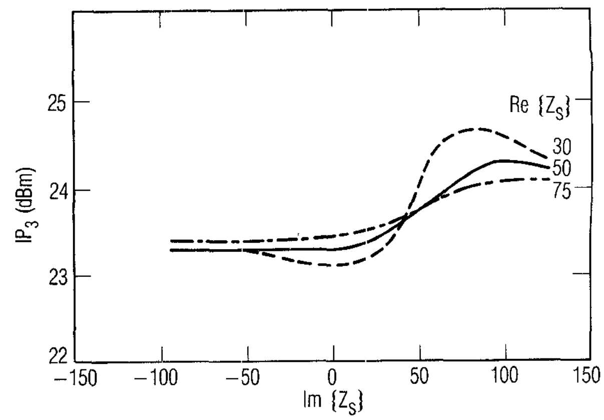


Fig. 8. Sensitivity of $IP_3$ to $Z_s$ at 5 GHz; $Z_L = 65 + j86$ (this is the optimum value of $Z_L$ when $Z_s = 50 + j0$).

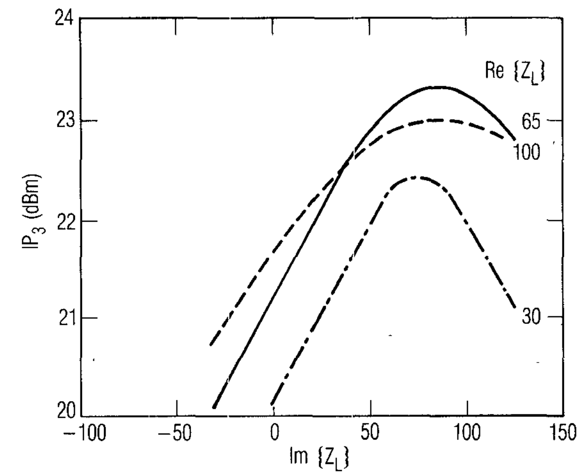


Fig. 9. Sensitivity of $IP_3$ to $Z_L$ at 5 GHz; $Z_s = 50 + j0$.

put circuit consisted of a quarter-wave transformer and a length of 50 Ω line. $\Gamma_s$ was varied by trimming the width of the microstrip transformer; thus its impedance increased each time it was cut. The output was conjugate matched in each case by means of a tuner, and intercept points were measured via a two-tone test. In this way, the intercept points for eight $\Gamma_s$ values were obtained.

The transformer's step-discontinuity reactances are an important component of $\Gamma_s$. Unfortunately, attempts to model these reactances via closed-form quasi-static approximations were not successful because of the limited accuracy of such formulations. To determine these values, we note that the dominant effect of the transformer is to change the magnitude of $\Gamma_s$, while the discontinuities primarily affect the phase. Thus, one can find $|\Gamma_s|$ from the transformer impedance, and $\angle\Gamma_s$ as the point where the $|\Gamma_s|$ curve intersects the gain circle. This heuristic approach treats the FET's measured $S$ parameters as a standard. This is reasonable, because the FET's $S$ parameters—measured by an accurately calibrated automatic network analyzer—are known more accurately than the discontinuity reactances.

The experimental intercept points and the calculated data are plotted on a Smith chart in Fig. 7; the gain and $IP_3$ values are corrected for the loss in the output tuner (0.7 dB). The difference between the calculated and measured $IP_3$ values in most cases is less than 1 dB.

At 10 GHz, the MESFET is unconditionally stable. It is evident from Fig. 6 that the intercept points in this case do not vary much along the gain circles, or even from one gain circle to another; the distortion levels are already minimal for unconditionally stable conditions. This insensitivity of $IP_3$ to $\Gamma_s$ is a characteristic of unilateral circuits [1]. We believe that the reason for the insensitivity of $IP_3$ to $\Gamma_s$ is a manifestation of the fact that feedback effects are minimal in an unconditionally stable circuit. Thus, in terms of its $IP_3$ characteristics, the amplifier behaves much like a unilateral circuit.

At 5 GHz the MESFET is conditionally stable and has optimum values of $\Gamma_s$ for minimizing third-order intermodulation distortion. Fig. 5 shows that the intercept points are highest near the counterclockwise extreme of the gain circles, and are nearly independent of gain. At the clockwise extreme, the intercepts are lower and are much more sensitive to gain; the $IP_3$ values increase as gain decreases. In general, the intercept points are lower in regions near the stability circle.

The same conclusions can be deduced from the 2 GHz case shown in Fig. 4, except that the effects are more pronounced. The best performance is obtained near the counterclockwise end of the gain circle, and the worst performance—a 12 dB reduction in $IP_3$—occurs near the clockwise end.

Figs. 8 and 9 show the sensitivity of $IP_3$ to source and load impedance when no gain constraint is imposed. It is clear from these figures that the intrinsic sensitivity of $IP_3$ to load impedance is much greater than the sensitivity to source impedance. (However, if $IP_3$ were defined in terms of available input power instead of output power, a definition that sometimes is more relevant, the sensitivity to $\Gamma_s$ would be greater.) This sensitivity to load impedance is reflected in the data of the earlier figures: at 10 GHz, where the FET is unconditionally stable and thus feedback effects are minimal, the value of $\Gamma_L$ that results in a conjugate match is close to $S_{22}^*$ and does not vary much as $\Gamma_s$ is varied. Consequently, the $IP_3$ does not vary significantly with $\Gamma_s$. However, at 5 GHz the FET is conditionally stable and $\Gamma_L$ varies more strongly with $\Gamma_s$; the sensitivity of $\Gamma_L$ to $\Gamma_s$ is especially severe at 2 GHz. It is interesting to note that the worst values of $IP_3$ are strongly associated with highly reactive values of $\Gamma_L$. These results are consistent with an experimental study of IM in MESFET's that identified $\Gamma_L \approx S_{22}^*$ as a good estimate of the load impedance that maximized $IP_3$ [14].

Fortunately, the values of $\Gamma_s$ that optimize intercept point are generally in the same region of the input plane as those that optimize noise figure. Thus, at a given bias level the trade-off between noise and linearity in a FET amplifier may not be very severe. However, the bias conditions that optimize noise figure ($I_d \approx 0.15 I_{dss}$) and those that optimize $IP_3$ ($I_d \approx 0.50 I_{dss}$) present a substantial trade-off.

## V. Conclusions

These results show that this approach to optimizing intercept points is practical and accurate. The measured and predicted intercept points fall within approximately 1.5 dB of each other, which is little more than the uncertainty in the measurements themselves. The use of a complete MESFET model makes the results particularly meaningful, because no significant effects related to the circuit topology (e.g., feedback phenomena) are ignored.

Under available-gain constraints, the MESFET's output $IP_3$ is sensitive to $\Gamma_s$. At low frequencies, where the MESFET is conditionally stable, the MESFET's $IP_3$ is most sensitive to $\Gamma_s$. However, as frequency is increased, that sensitivity decreases and essentially disappears at the point where the MESFET becomes unconditionally stable. This sensitivity is the result of feedback effects that cause the conjugate-match $\Gamma_L$ to be highly reactive. When gain constraints are removed, the sensitivity of output $IP_3$ to $\Gamma_L$ is greater than the sensitivity to $\Gamma_s$.

Conventional methods of modeling the drain-current nonlinearity do not include potentially significant effects in the device. Further research is needed to develop more accurate modeling techniques.

## Acknowledgment

The authors would like to thank G. Stout and W. Yamada for assistance with the S-parameter measurements, R. Gowin for assistance with the fabrication of test fixtures, W. Garber for some of the dc device measurements, and M. Meyer for reviewing the manuscript.

## References


[1] S. Maas, *Nonlinear Microwave Circuits*. Norwood, MA: Artech House, 1988.

[2] R. Gilmore, "Nonlinear circuit design using the modified harmonic-balance algorithm," *IEEE Trans. Microwave Theory Tech.*, vol. MTT-34, p. 1294, 1986.

[3] W. R. Curtice, "Nonlinear analysis of GaAs MESFET amplifiers, mixers, and distributed amplifiers using the harmonic balance technique," *IEEE Trans. Microwave Theory Tech.*, vol. MTT-35, p. 441, 1987.

[4] V. Rizzoli, C. Cachetti and A. Lipparini, "A general-purpose program for the analysis of nonlinear microwave circuits under periodic excitation by multidimensional Fourier transform," in *Proc. 17th European Microwave Conf.*, 1987, p. 635.

[5] R. S. Tucker, "Third-order intermodulation distortion and gain compression in GaAs FETs," *IEEE Trans. Microwave Theory Tech.*, vol. MTT-27, p. 400, 1979.

[6] R. K. Gupta, L. G. Englefield, and P. A. Goud, "Intermodulation distortion in microwave MESFET amplifiers," in *IEEE MTT-S Int. Microwave Symp. Dig.*, 1978, p. 405.

[7] R. A. Minasian, "Intermodulation distortion analysis of MESFET amplifiers using the Volterra series representation," *IEEE Trans. Microwave Theory Tech.*, vol. MTT-28, p. 1, 1980.

[8] G. M. Lambrianou and C. S. Aitchison, "Optimization of third-order intermodulation product and output power from an X-band MESFET amplifier using Volterra series analysis," *IEEE Trans. Microwave Theory Tech.*, vol. MTT-33, p. 1395, 1985.

[9] A. M. Crosmun, "Use of Volterra series analysis for optimizing the intercept point of GaAs MESFET small-signal amplifiers," M.S. thesis, UCLA, Los Angeles, CA, 1988.

[10] S. A. Maas, "A general-purpose computer program for the Volterra-series analysis of nonlinear microwave circuits," in *IEEE MTT-S Int. Microwave Symp. Dig.*, 1988, p. 311.

[11] L. Yang and S. I. Long, "New method to measure the source and drain resistance of the GaAs MESFET," *IEEE Trans. Electron Devices*, vol. EDL-7, p. 75, 1986.

[12] A. Fukai *et al.*, "Determination of GaAs MESFET parasitic resistances by using the gate 'current-crowding' technique at linear drain biases," Aerospace Corp. Technical Memorandum No. ATM-87(8268)-1, 1987.

[13] S. A. Maas and A. M. Crosmun, "Modeling the gate *I/V* characteristics of a GaAs MESFET for Volterra-series analysis," *IEEE Trans. Microwave Theory Tech.*, vol. 37, pp. 1134–1136, July 1988.

[14] C. Y. Ho and D. Burgess, "Practical design of 2–4 GHz low intermodulation distortion GaAs FET amplifiers with flat gain response and low noise figure," *Microwave J.*, vol. 26, p. 91, Feb. 1983.


**Andrea M. Crosmun** (M'89) was born in Nuremburg, Germany, on December 24, 1962. She received the B.S. degree in 1985 and the M.S. degree in 1988 in electrical engineering from the University of California, Los Angeles, where she is currently working towards the Ph.D. degree.

From July 1985 to October 1987 she was with the Ground Systems Group, Hughes Aircraft Company, designing passive microwave circuits. Since October 1987 she has been with The Aerospace Corporation, Los Angeles, CA, involved primarily in researching the nonlinear effects in GaAs FET devices.

Ms. Crosmun is a member of Eta Kappa Nu and Tau Beta Pi.

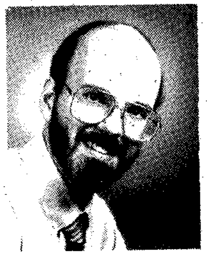

**Stephen A. Maas** (S'80–M'83) was born in Quincy, MA, in 1949. He received the B.S.E.E. and M.S.E.E. degrees in electrical engineering from the University of Pennsylvania in 1971 and 1972, respectively, and the Ph.D. degree in electrical engineering from the University of California, Los Angeles, in 1984.

He has been involved in the research and development of low-noise and wide-dynamic-range receiving systems and components for radio astronomy and space communication at the National Radio Astronomy Observatory, Hughes Aircraft Company, and TRW. His primary research interests involve the optimization of nonlinear microwave circuits, especially by means of Volterra-series techniques. He is currently a Research Scientist at The Aerospace Corporation, Los Angeles, CA, teaches periodically at UCLA, and consults for companies in the Los Angeles area.

Dr. Maas is the author of two books: *Microwave Mixers* (Artech House, 1986) and *Nonlinear Microwave Circuits* (Artech House, 1988).